SEDIMENTATION AND EARLY DIAGENESIS OF THE CAVERNOUS LIMESTONE (RÖTH) OF GOGOLIN, SILESIAN-KRAKÓW REGION, POLAND

Adam Bodzioch[1] & Stanisław Kwiatkowski[2]

[1] *A. Mickiewicz University, Institute of Geology, ul. Maków Polnych 16, 61-606 Poznań, Poland*

[2] *Polish Academy of Sciences, Institute of Geology, ul. Senacka 1, 31-002 Kraków, Poland*

A b s t r a c t : The horizon of Cavernous Limestone occurs at the Lower/Middle Triassic boundary of the Silesian-Kraków region. It consists mainly of dedolomites and peloidal grainstones in which numerous calcitic pseudomorphs after gypsum and halite, siliceous nodules, microbial mats, tepee structures, fenestral fabrics, small wave ripples and erosional features were found. These features and calcareous microfacies indicate that the sediment was deposited in supralittoral ponds supplied occasionally with normal salt sea waters. There were therefore periods of slow evaporation when lime mud undergoing rapid pelletization was deposited. With increasing salinity, the gypsum and halite crystallized, surficial dolomitization and a selctiv silicification of algal mats and of early diagenetic sulfate nodules occurred. During affluence of normal sea waters, the surficial sediment was eroded and allochthonous, grained material consisting of peloids, oncoids, bioclasts and detrital quartz was deposited. As a result of decreasing salinity dissolution of evaporitic minerals and induced calcificacion of the sediment took place. The temperature and pH lowered inducing precipitation of silica. The next evaporite cycle resulted besides in the redolomitization of sediment and crystallization of fibrous gypsum in vugs which remained after dissolved halite.

K e y   w o r d s : supralittoral environment, pseudomorphs after evaporitic minerals, dedolomite, microbial mats, silicification, dolomitization, Lower Triassic.

INTRODUCTION

The term "Cavernous Limestone" is used to describe strongly porous, re-crystallized, brown limestones containing numerous siliceous nodules in the Triassic sediments of the Silesian - Kraków area (Fig. 1) (Eck, 1865; Ahlburg, 1906; Assmann, 1913, 1933; Doktorowicz-Hrebnicki, 1935; Siedlecki, 1949, 1952). These limestones occur at the Röth/Muschelkalk boundary and they
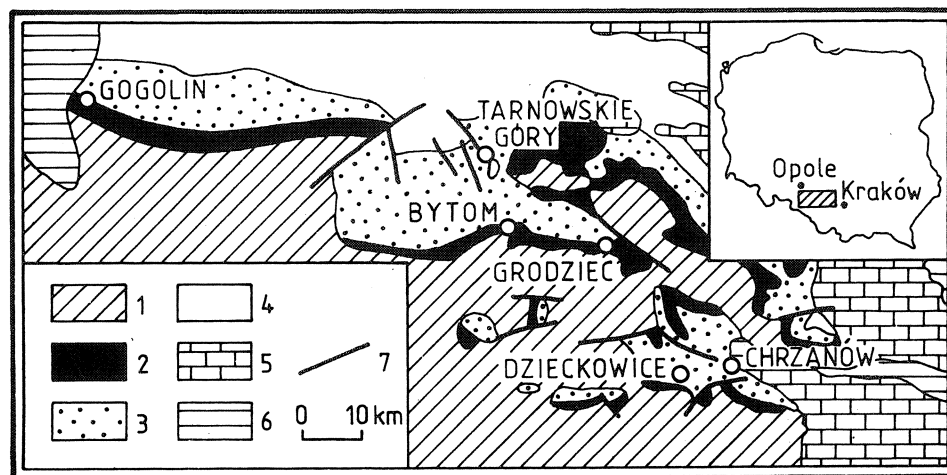
Fig. 1   Geological map of Silesian-Kraków region. *1* – Palaeozoic, *2* – Buntsandstein, *3* – Muschelkalk, *4* – Keuper, *5* – Jurassic, *6* – Cretaceous, *7* – faults

form a discontinuous lithostratigraphical horizon (Siedlecki, 1952). The maximum thickness of the Cavernous Limestone reaches about 12 m in the vicinity of Bytom (Eck, 1865; Assmann, 1913, 1933).

The investigations of Cavernous Limestone here presented were carried out in Gogolin, in an old abandoned quarry which is situated rightside the road leading from Gogolin to Goraźdźe (Fig. 2). At this place, about 1.5 m thick topmost part of the Röth can be observed (Fig. 3). The bottom of the sequence can not be seen but light grey pelitic limestones with molluscs and echinoderms lying above are well outcropped. These limestones belong to the Gogolin Beds (lowermost Muschelkalk).

Field and laboratory works were made in the years 1990-1991. For reconstruction of sedimentary processes and diagenesis of Cavernous Limestone, the carbonates were analysed (A. Bodzioch) as well as silica bodies (S. Kwiatkowski) on the ground of 40 thin sections stained with standart methods (Friedman, 1959; Dickson, 1966; Evamy, 1969) and 40 polished surfaces. Moreover, 4 diffraction and 13 SEM analyses were done.

DESCRIPTION

The Cavernous Limestone outcropped at Gogolin consists mainly of thin-layered, thoroughly recrystallized limestones, yellow, red and brown, accompanied by thin layers of pelitic and grain-supported limestones. Apart from characteristic vugs and siliceous nodules, a lot of various calcitic pseudomorphs after gypsum, anhydrite and halite have been found together with microbial mats, tepee structures, fenestral fabrics, wave ripples, erosional cuts and microfossils (foraminifers and ostracods), trace fossils of *Planolites* type
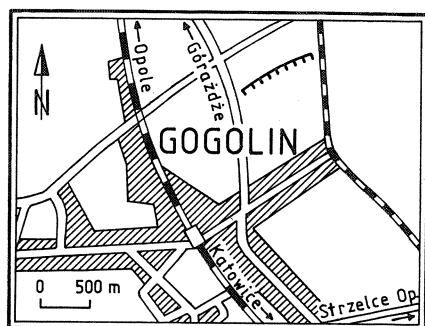
Fig. 2   Position of Cavernous Limestone outcrop in Gogolin

and calcitized fragments of bones. The sediment consists predominantly of low-Mg calcite and contains locally dispersed Ca-sulfates (revealed by diffraction analysis).

VUGS

There occur two principal types of vugs. The first one is represented by oval pits reaching the length of 50 cm and the height of 30 cm (Pl. I: 1). They occur in the upper part of the section where they form distinct horizons. The pits are empty or filled with breccias consisting of fragments of stromatolitic and crystalline limestones. The second, more frequent type of vugs is represented by strongly flattened lenticular vugs which are internally subdivided into sharply ridged cells by thin vertical or diagonal calcitic walls (Pl. I: 2-5). The walls are calcitic pseudomorphs after discoidal gypsum (Pl. I, fig. 2), fibrous gypsum (Pl. I: 3), or they are recrystallized sediment remaining between firstly dissolved and then removed crystals of halite (Pl. I: 4) and other evaporitic minerals (Pl. I: 5). The cells are empty or partly filled with very fine crystalline, poorly consolidated sediment resembling "sandyficated" limestones and dolomites well known from the Karchowice Beds (Lower Muschelkalk) of the Upper Silesian region (Dżulyński & Kubicz, 1971). The occurrence of cellular zones is not regular, however they tend to concentrate along less or more distinct horizons in top parts of layers of crystalline limestones. In cellular parts of the sediment, a characteristic intracrystalline porosity has developed (Pl. I: 6). The pores occur within relicts of zoned crystals of halite in which halite was removed and only intercalations of sediment were preserved. All vugs represent early diagenetic solution enlarged mouldic porosity type (Choquette & Pray, 1970) which is the result of dissolution of evaporitic minerals.

MICROFACIES

Two main types of limestone microfacies can be distinguished in the studied sequence: peloidal grainstones represented by pelitic sediment and dedolomites represented by crystalline limestones.

Peloidal grainstones

The sediment distinguished as the peloidal grainstones microfacies consists
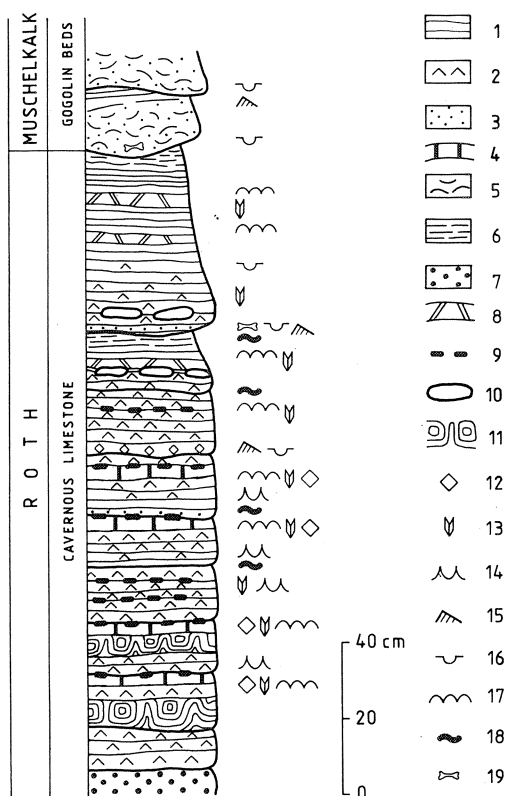
Fig. 3   Stratigraphical column of Cavernous Limestone in Gogolin. *1* – pelitic limestones, *2* – crystalline limestones, *3* – grained limestones, *4* – cellular limestones, *5* – coquina, *6* – marls, *7* – sandstones, *8* – collapse breccia, *9* – chert nodules, *10* – caverns, *11* – layers of displacive halite, *12* – pseudomorphs after halite, *13* – pseudomorphs after gypsum, *14* – tepee structure, *15* – ripplemarks, *16* – erosional cuts, *17* – algal mats, *18* – Planolites, *19* – remains of vertebrates

of oval peloids (McKee & Gutschick, 1969) which are built of micrite and do not display any internal structure (Pl. II: 1). Peloids are relatively small (0.03-0.15 mm) and poorly sorted. They are accompanied by foraminifers (Pl. II: 2, 3) and ostracods (Pl. II: 4). Individual peloids are well visible and they are sharply bounded where they contact with cement (Pl. II: 1, 3, 4). The calcitic pseudomorphs after single, small, euhedral crystals of dolomite growing toward the interior of rhomboidal pores surround peloids (Pl. II: 1, 5). The remaining pore space is filled with blocky sparite which extinguishes light under crossed nicols together with the pseudomorphs after dolomite.

This sediment is intercalated by poorly distinguishable thin micritic laminae. Boundaries between peloids are not distinct and individual peloids can be distinguished only sporadically (Pl. II: 2, 3). Instead, one can see a lot of small, oval vugs filled with blocky calcite and developed parallel to lamination (birdseye structures - Pl. II: 6). Their horizontal development and presence of true algal mats suggest that they formed as a result of gas bubbles due to decay of organic matter (cf. Shinn, 1968, 1983b).

Peloidal sediment displays no indicators of hydrodynamical influence (e.g. ripples, erosional cuts, cross- or gradual bedding, sorting etc.). Therefore, we can conclude that peloids were formed in situ. Their shapes and sizes differ from both fecal pellets (e.g. Cloud, 1962; Bathurst, 1975) and grains precipitating directly from sea water (e.g. MacIntyre, 1985; Chafetz, 1986). On the other hand, their concurrence with birdseye structures indicates that peloids, as well as grainstone texture, formed by pelletization of the lime mud due to

migration of gases originated by decay of organic matter (cf. Mazzullo & Birdwell, 1989).

Another problem is that of pseudomorphs after small euhedral crystals of dolomite. The position of crystals around peloids suggests that dolomite was the first generation of cement (cf. Carballo et al., 1987; Lasemi et al., 1989) which could precipitate directly from pore waters (e.g. Shinn et al., 1969; de Groot, 1973). It seems that growing of crystals of dolomite changed the primary shapes of pores into rhomboidal, in contrast to rhombohedral pores developing during dedolomitization (Evamy, 1967). Syntaxial extinction of light by blocky sparite and pseudomorphs after dolomite may indicate that the origin of pseudomorphs was closely connected with precipitation of calcite cement. Probably, the change of chemical composition of pore waters caused simultaneously replacing of dolomite by calcite and precipitation of the second generation cement.

Dedolomite

Crystalline limestones are the main component of the sediment described. They are built of a mosaic of xenomorphic calcite crystals and show several features typical for dedolomitization processes. First of all, they are calcitic pseudomorphs after sucrosic xenotopic dolomite (sensu Friedman, 1965; or nonplanar sensu Sibley & Gregg, 1987), (Pl. III: 1), relicts of dissolved dolomite being preserved inside pseudomorphs or at their boundaries and formed some kind of grumeleuse (clotted) structure (Beales, 1965; Bathurst, 1975; Evamy, 1967) (Pl. III: 1, 2), and rhombohedral areas which extinguish under crossed nicols inconsistently to their outlines (cf. Podemski, 1973; Peryt, 1984; Theriault & Hutcheon, 1987). Inside of large calcite crystals originated during dedolomitization, calcitic pseudomorphs after small euhedral dolomite crystals occur (Pl. III: 3). Primary grains are usually preserved as poorly distinguishable relicts, however it is possible to distinguish remains of peloids (Pl. III: 2), oncoids (Pl. III: 1), foraminifers (Pl. III: 4) and ostracods (Pl. III: 5). Non carbonate grains are represented by fragments of vertebrate skeletons (Pl. III: 6), mica and detrital quartz. They are concentrated together with carbonate grains in thin allochthonous laminae with erosional bottom surfaces (Pl. IV: 2). Moreover, pseudomorphs after small crystals of gypsum and anhydrite are very frequent. Locally, a very dense fenestral fabric is present as horizontal to vertical, anastomozing vugs filled with blocky calcite (Pl. IV: 1). This fabric strongly resembles an alveolar texture (Esteban, 1974) both in shape and size of pores. Therefore, we can interpret this texture as the product of coalescent millimetre-sized rhizoliths (cf. Steinen, 1974; Klappa, 1980; Esteban & Klappa, 1983).

PSEUDOMORPHS AFTER EVAPORITIC MINERALS

Calcitic pseudomorphs

Within the studied sediment, calcitic pseudomorphs after needle-shaped crystals of gypsum and anhydrite, discoidal and fibrous gypsum, after laminated gypsum crusts and halite have been found.

Pseudomorphs after small crystals of gypsum are dispersed within the sediment in top parts of dedolomite layers (Pl. IV: 4), as well as pseudomorphs after anhydrite (Pl. IV: 3). They occur just beneath the horizons containing siliceous nodules or within them. The length of needle-shaped crystals never exceeds 1 mm. They form several mm thick laminae in which they are randomly oriented – these features suggest crystals' growing within the sediment. In such layers, there is a regularity in the arrangement of components of the sediment. In lowermost parts of layers peloids predominate but towards the top, the number of peloids gradually decreases while at the same time the number of pseudomorphs after gypsum and sucrosic dolomite increases significantly. Moreover, the number of pseudomorphs after gypsum is proportionally related to the volume of pseudomorphs after dolomite. This vertical variability shows the upward increasing intensity of both dolomitization and crystallization of gypsum, and it indicates an upward increasing concentration of brines which filled pores in sediment. It leads to the conclusion that dolomitization was only a surficial process which seems to become less intense deeper in the sediment. The relation between the volume of pseudomorphs after dolomite and gypsum suggests that dolomitization developed due to the increase in Mg/Ca ratio (cf. Folk & Land, 1975) caused by crystallization of gypsum (cf. Butler, 1969; Patterson & Kinsman, 1982; Hardie, 1987). Owing to the vertical gradient of concentration of brines, the surficial sediment was totally replaced by dolomite while several centimetres below it the peloidal grainstone texture was preserved and only the dolomite cement precipitated.

The process of calcitization of the sediment remains still unclear, however there are two points to discuss: the presence of pseudomorphs after gypsum and anhydrite (1), and the vertical variability in the intensity of calcitization which is analogous to the variability in the intensity of dolomitization (2). The former indicates that dissolution of sulfates could be the source of Ca-ions (e.g. Back *et al.*, 1983; Theriault & Hutcheon, 1987), and the latter – that dedolomitization was a surficial process only, like dolomitization (cf. Evamy, 1967; de Groot, 1967). Such a process caused in the surface sediment total replacing of the pre-existing dolomite by large, xenomorphic crystals of calcite, whereas within peloidal grainstones lying just below it caused only precipitation of blocky sparite cement and calcitization of the earlier dolomite cement. Pseudomorphs after dolomite rhombs occurring inside large calcite crystals formed during dedolomitization indicate that firstly calcitized rocks were later dolomitized and calcitized once more. The intensity of redolomiti-

zation and recalcitization seems to be relatively low - they did not cause large-scale recrystallization of the rocks formed earlier.

Pseudomorphs after discoidal crystals of gypsum occur in cavernous parts of the sediment where these crystals form walls and cells (Pl. I: 2). In plane, they form more or less regular polygons (Pl. V: 1). Shapes of these pseudomorphs indicate rapid crystallization of gypsum from highly concentrated brines (cf. Deicha, 1943), which were alkaline and rich in organic compounds (Cody, 1979; Kirov, 1980). The polygonal arrangement of crystals may be a result of crystallization in desiccation cracks (cf. Schreiber et al., 1986) or in fissures originated by sediment contraction due to dolomitization (cf. Friedman & Sanders, 1967; Shinn, 1973).

Pseudomorphs after fibrous gypsum occur only in relatively small, irregular vugs where they form internal walls (Pl. I: 3).

Calcitic pseudomorphs after laminated crusts have been found in dedolomite layers where they occur on the upper surface of allochtonous laminae (Pl. VI: 4). Crusts are several mm thick and they are built of calcitized, vertically oriented crystals of gypsum. Within crusts submillimetric laminae of micrite occur. They separate particular layers of this structure and cross-cut vertically oriented crystals of calcite. Excluding calcitization and small sizes of primary crystals of gypsum, they are very similar to vertically oriented selenite (cf. Hardie & Eugster, 1971; Schreiber & Kinsman, 1975; Vai & Ricci-Lucchi, 1977; Warren, 1982). They are interpreted as a result of competitive growth of selenite from a depositional surface in shallow hypersaline waters (cf. Schreiber & Kinsman, 1975), however, vertically oriented crystals of gypsum are also known from biolaminated sulfates deposited in subaerially exposed settings (Gerdes & Krumbein, 1987). In the discussed case, the occurrence of crystals on the top surfaces of hydrodynamically deposited sediment speaks rather for the first interpretation. Micritic laminae between horizons of gypsum evidence episodes of lime mud deposition during the periods of lower salinity (cf. Hardie & Eugster, 1971; Schreiber & Kinsman, 1975; Warren, 1982). Possibly syntaxial overgrowth of gypsum incorporating micrite laminae is marked by vertical orientation of calcite crystals which most probably replaced large, multiple crystals of gypsum.

Calcitic pseudomorphs after halite occur inside some cells (Pl. I: 4) where they are preserved in situ, and on rippled bottom surfaces of dedolomite layers (Pl. V: 2), where the primary crystals of halite had been redeposited (e.g. West et al., 1968; Karcz & Zak, 1987). Independently of the mode of occurrence, there are randomly oriented idiomorphic crystals of sizes up to 2 cm. All crystals display a hopper structure (Arthurton, 1973), i.e. they posses concave walls with clearly visible accretion rings (Pl. VI: 1). Crystals are built of blocky calcite containing relicts of dedolomite sediment and forming with them thin intercalations (Pl. VI: 2). Individual crystals of calcite extinguish light under crossed nicols together with parts of sediment occurring both inside and outside them (Pl. VI: 3). Primary sediment/halite intercalations

suggest that crystallization of halite took place episodically within the sediment (cf. Gornitz & Schreiber, 1981). On the other hand, the hopper structure of crystals indicates their rapid growth from supersaturated brines, possibly in the case of rapid evaporation (cf. Arthurton, 1973; Southgate, 1982). The mode of light extinction suggests that the origin of pseudomorphs was closely connected with calcitization of the sediment – calcite crystals must have simultaneously replaced both evaporites and dolomite sediment.

Besides pseudomorphs, crystals of displacive halite are also common (Pl. I: 4, 6; Pl. VI: 5, 6). They are built of laminae of dedolomite between which vugs remaining after dissolved halite form the intracrystalline porosity (Pl. I: 6). Growth of such crystals took place within the sediment when crystallization of halite alternates with its dissolution.

Silicified anhydrite nodules

These nodules occur in a bed of yellow and brown limestone, sandy, laminated, stained with organic pigment, with skeletal remains (foraminifers) and with dark brown balls (algae ?). This bed is divided (from bottom upwards) in the following layers (Pl. VII: 1):

A – limestone, medium-grained, sandy,

B – limestone, coarse-grained, sandy, stained with horizontal setting of grains and of organic pigment bands,

C – limestone, coarse-grained, sandy, with skeletal remains, with less distinct horizontal setting of constituents,

D – limestone, fine-grained, sandy, with constituents not in horizontal position,

E – limestone, laminated (laminae 1.3-3.5 mm thick); light, coarse-grained laminae alternate with dark fine-grained laminae, the thickness of coarse-grained laminae diminishes upwards.

The siliceous nodules occur in layer B and in the lower part of layer C. They are irregular, nebulous, 12-40 mm long, 8-20 mm thick. They are formed by gray silica, surrounded by white silica, with dispersed fragments of brown limestone. Silica is pure, with rare small strings of brown pigment. It is formed by length-slow chalcedony, and more rarely by length-fast chalcedony.

There occurs commonly the "pile of bricks" texture (Carozzi, 1972), composed of rectangular, brick-shaped grains (Pl. VII: 2). These rectangular grains of various length and width are often set under right angle one to another or are forming fans. Locally they bifurcate, and locally they are divided by rosettes of length-slow or length-fast chalcedony. In many medium and coarse "bricks" their structure is visible, composed of small, parallel quartzine crystals, perpendicular to the long axis of the "brick". There occur algal fibres, preserved in chalcedony.

The "pile of bricks" texture is characteristic for silicified anhydrite crystals (West, 1964; Carozzi, 1972). The occurrence of length-slow chalcedony as

principal form of silica confirms that these nodules were primarily built by anhydrite (Folk & Pittman, 1971; Milliken, 1979; Arbey, 1980). The top surface of layer C is lifted over the nodules. The layer D covers the uneven top of layer C, and its top is even and almost horizontal. Theoretically this structure either resulted from compaction – greater in calcareous deposit and lesser in silica nodule, or it was formed by growth of anhydrite nodules in the deposit which uplifted the overlying layer C. The replacement of anhydrite nodules by silica did not form the hollow geodes or the cauliflower nodules, which occur commonly in this type of deposits (Chowns & Elkins, 1974).

Apart from described nodules there are in Gogolin Cavernous Limestone many siliceous nodules (up to 1 cm thick) formed by white silica. They contain no "pile of bricks" structure, but often length-slow and zebraic chalcedony and lutecite. The presence of these minerals suggests that they are formed by silicification of sulfates (Arbey, 1980).

MICROBIAL MATS

Carbonate microbial mats

Algal mats and related structures occur in the whole section, however they are usually badly preserved as cryptalgal fabrics sensu Aitken (1967) (Pl. VIII: 1). Within them, nodular bodies occur, consisting of very fine crystalline, poorly consolidated calcite – probably calcitized anhydrite nodules. Better preserved stromatolites contain a lot of remains of algal filament, as well as relatively large fenestrae filled with calcite or silica. Locally small -scale collapse breccias are present in the internal vugs (Pl. VIII: 3), and the upper surfaces of algal laminae are cracked (Pl. VIII: 4). In depressions of vugs crystalline calcitic silt is preserved (Pl. VIII: 2). The same silt infills also the interior of algal filament. The remaining pore spaces are filled usually with two generations of sparite (Pl. VIII: 2-4) or with silica. The first generation of calcite cement is represented by medium-sized granular cement which covers the surface of vugs, crystalline silt and crumbs of breccias; the second generation - by very coarse crystalline, blocky sparite. In the few pores filled with silica the first generation of calcite cement is absent while the second generation occurs only in fissures cutting the silica bodies (Pl. VIII: 2).

Although thin smooth algal mats which cover carbonates containing quartz and evaporites are known mainly from tidal flats (Kendall & Skipwith, 1968; Benkes & Lowe, 1989), a direct interpretation of described microbial mats is not possible. It is easier to establish the sequence of diagenetic events; however, the nature of crystalline silt and silica infillings is not quite clear. In vue of the above described features of the sediment, it is possible to conclude that both the silt and silica are the remainings after evaporite minerals, most probably anhydrite, which was dissolved in the case when silt was formed or replaced in the case of silica formation.

Cracking of the upper surfaces of microbial laminae is the first well evidenced process of diagenesis. It may have resulted from drying of microbal mats, growing of anhydrite nodules, or from both of these processes which could take place at the same time. In the next step of diagenesis, anhydrite was dissolved or replaced by silica, indicating a change in the chemical composition of pore waters, and collapse breccias formed. Then the first generation of calcite cement precipitated. After it there was compaction and precipitation of the second generation of sparite.

Silicified microbial mats

The presumable microbial mats occur in the yellow, yellow-red or red limestone, locally mottled, irregularly laminated, usually cavernous. The vugs are horizontal, long and thin (1-7 mm high, long to 60 mm). There occur bands of similar dimensions with numerous, small pores (0.1-2.0 mm). In places the limestone is not cavernous and not porous. It consists principally of sparite and contains small grains of detritic quartz, nests of coarse calcite crystals and some rings of biogenic origin (algae). It is irregularly stained with brown organic pigment. On the wavy top surface of this limestone there are siliceous bodies (Pl. IX and X) in the form of small plates (1-30 mm diameter, ca 1 mm thick), flat or weakly convex upward. Horizontally they are circular, oval, beans-shaped, triangular or rectangular with rounded corners, or deformed "8"-like. In some cases the plates are divided and form flat-topped mounds. The plates are surrounded by a single, exceptionally double, ring, 1-3 mm wide, usually higher than the plate, sometimes lower. Between plate and ring there is a thin groove. The rings of neighbouring plates are often connected continuously. In places the plates and rings are partly covered by limestone and there the rings are not visible. The bottom surface of plates and rings is flat or very slightly concave and between plate and ring there is also a thin groove. These plates and rings do not cover the whole top surface of the bed. In particular areas they cover from 0 to 80% of the surface, usually about 15%. In the areas without the plates and rings there are many pseudomorphs after gypsum crystals (up to 24 mm long). Single, rare pseudomorphs occur also between the plates. Beneath the top surface there occur not numerous, single plates with rings. Both the plates and rings are formed by gray chalcedony, uniform, fine and evengrained.

The shape of these siliceous bodies suggests that they are a silicified microbial mat. They are very similar to the siliceous bodies described as blue green algae mat from Aleman Formation, New Mexico (Geeslin & Chafetz, 1982). A Recent mat of blue green alga Lyngbya in Laguna Mormona in Baja California, Mexico (Horodyski, 1977) has on the surface flat-topped mounds and rings, somewhat similar to our forms. The small, flat-topped mounds with composite rings described by Carozzi (1962) from the recent algal mat in Salt Lake, Utah, are similar to our forms, but they are some tens times larger. The

thinness of the plates and rings indicates extremely shallow water at the time of algal life. The silicification is limited to the algal mat, which was especially susceptible to it, with surrounding carbonate mud non silicified. This selective silicification was possible in an early stage of diagenesis, when the organic matter of algae was yet not quite destroyed.

COLLAPSE BRECCIAS

Apart from breccias in stromatolites, there are also present collapse breccias forming layers several centimetres thick and of lateral extent reaching tens of metres (Pl. XI: 1). They are built of crushed fragments of microbial mats floating in crystalline calcite (Pl. XI: 2). Sparite cements are identical as in stromatolites (Pl. XI: 3). It is clearly visible here that the second generation of sparite is late postcompactional.

TEPEE STRUCTURES

Problematical tepee structures occur locally in the lower part of the sequence. They form large, more or less regular polygons with diagonal lines up to 1 m long (Pl. XI: 4, 5). These structures consist of anticlinally deflected stromatolitic layers several centimetres thick. The depressions between anticlines are filled partly with fine crystalline calcitic sediment in which trace fossils of *Planolites* type occur (Pl. XI: 6). Shapes of these structures resemble embryo tepees (Assereto & Kendall, 1977), and their concurrence with cellular limestones recalls boxwork tepees (Kendall & Warren, 1987). On the other hand, the presence of microbial mats, as well as their somewhat crinckled patterns show a similarity to the so called "petee" structures (Gerdes & Krumbein, 1987). It seems that the described structures formed due to consolidation of the sediment by microbial slime, and to subsequent expansion of the sediment crust caused by pressure of evaporitic minerals crystallized beneath.

CHERT LAYERS AND LAMINAE, AND SILICO-CALCAREOUS NODULES

The chert layers and laminae form the intercalations in the limestone beds. The chert layers (1-2 cm thick) are formed by dark-gray silica with thin white silica rims at top and bottom of the layer (Pl. XII: 1). The chert shows vertical cracking. The lower boundary of the chert is uneven, the upper one is even. Chert consists of microcrystalline quartz with dispersed grains of length-fast chalcedony. Length-slow chalcedony is absent. Lutecite was observed in skeletal remains. The chert contains numerous ostracods and spores and occasionally foraminifers, small brachiopods and pelecypods. The limestone underlying chert is cavernous and it is devoid of detritic quartz. The limestone overlying chert has no vugs and contains detritic quartz.

The chert laminae (0.5-1 mm thick) consist of white silica (quartz and rarely length-slow chalcedony). They are wavy and locally discontinuous.

The silico-calcareous nodules form irregular flattened ellipsoids (up to 6 cm long), set in horizontal rows (Pl. XII: 2). Their interior consists of limestone with numerous white silica aggregates surrounded by thin rims of white silica. Silica occurs as quartz. Length slow chalcedony, zebraic chalcedony and lutecite are absent. The position of nodules in the rock is similar to that of chert layers and laminae. The underlying limestone is cavernous, without detritic quartz, the overlying one contains detritic quartz but no vugs.

The chert layers and laminae and silico-calcareous nodules in Gogolin Cavernous Limestone were described in detail in a paper by one of the present authors (Kwiatkowski, 1991), who believed that in a dry season the evaporites were precipitated and silica gels were agglomerated under conditions of high salinity, temperature and pH, and that there followed a period of flooding by sea water when temperature and pH dropped rapidly and the silica gels precipitated.

TUBULAR SILICA BODY

In a cavernous limestone bed there is a siliceous nodule with vertical tubular protuberance 17 mm high (Pl. XII: 3). The walls of this protuberance are formed by white silica and the center filled with porous limestone. At the outer surface of the protuberance walls there are imprints of very thin lamination, which probably existed in the surrounding carbonate sediment, but which was later destroyed.

Similar forms were interpreted as resulting from gazeous escape in a still plastic deposit (Maglione, 1979, pl. 8: 2) or as silicified gypsum tubes, formed on the plant stems (Bustillo & Diaz Molina, 1980). Other interpretations are: burrow filling or diapiric movement upwards of plastic silica.

INTERPRETATION

Typically developed layers of the Gogolin Cavernous Limestone consists of thin recurrent sequences. Each of them begins with peloidal grainstones which gradually change into dedolomite. Dedolomites reveal erosional surfaces and contain amounts of pseudomorphs after gypsum increasing upwards. The top of a completely developed sequence is built of cavernous limestones rich in pseudomorphs after halite and discoidal gypsum. These sequences were separated by thin allochthonous layers of dedolomite rich in detrital quartz, bones, oncoids, bioclasts and pseudomorphs after redeposited crystals of halite, and they usually formed in wave ripples. Some of these sequences begin with laminated crusts composed of vertically oriented pseudomorphs after gypsum. The development of such sequences took place in predominantly subaqueous conditions, as indicated by the marine fauna, wave

ripples, washed out surfaces, precipitation of lime mud and vertical growth of gypsum. On the other hand, we have also found some evidence for subaerial exposure of the sediment – alveolar fabrics, birdseyes, problematical tepees, and for very early, penesynsedimentary diagenesis – peloidal grainstone textures, dolomitization and calcification of the sediment, silicification. Repeatedly occurring changes in the chemical composition of pore waters are clearly documented by displacive halite, multiple dolomitization and calcitization, and various types of gypsum. Such changes occurred also in waters above the sediment surface, as indicated by gypsum/lime mud intercalations within the laminated crusts. These observations suggest that diagenetic processes were very closely connected with sedimentary events.

Most of the described features of the Cavernous Limestone is diagnostic for perilittoral settings, especially if they occur together (cf. Esteban & Klappa, 1983; Shinn, 1983a; Schreiber et al., 1986). The type of sedimentary and related diagenetic cycles indicates a very shallow-water, salinar environment where both physical and chemical conditions changed regularly. Recently, such conditions are known mostly from supralittoral ponds flooded by normal sea waters during tides or storms (cf. Kendall & Skipwith, 1969; Purser & Evans, 1973; Friedman & Krumbein, 1985; Warren & Kendall, 1985). Thus, we can reconstruct the sedimentary and diagenetic history of the sediment in the following sequence:

1. Deposition of lime mud at the bottom of a pond filled with sea water of normal salinity and the development of microbial mats.

2. Pelletization of lime mud owing to migration of bubbles of gases produced by decomposition of microbial mats. Simultaneously progressing evaporation leads to increase in salinity and to a decrease in the depth, which had the following consequences:

a – crystallization of needle-shaped gypsum inside the surface sediment and of vertical oriented gypsum crystals at its surface

b – dolomitization of the surface sediment due to crystallization of gypsum

c – precipitation of the dolomite cement in the pelleted sediment lying beneath the zone of intense dolomitization

d – dissolution of detritic quartz grains and polymerization of silica solutons

e – slight erosion of the surface sediment due to the lowering of the wave base

3. Complete or almost complete dessication of pond:

a – forming of dessication cracks and crystallization of discoidal gypsum within them

b – crystallization of anhydrite within and beneath microbial mats, cracking of their upper surfaces

c – forming of alveolar fabrics due to penetration of the sediment by plant roots

d — crystallization of halite

e — silicification of microbial mats and of anhydrite nodules

4. Inflow of normal sea water:

a — erosion of the surface sediment and deposition of the allochthonous layer

b — precipitation of silica gels

c — dissolution of evaporitic minerals in the surface layer of the sediment; forming of crystalline silt

d — dedolomitization through the supply of Ca-ions liberated from dissolved sulfates

e — calcitization of not dissolved evaporitic minerals

f — precipitation of the first generation of calcite cement, calcitization of the dolomite cement in peloidal grainstones

5. The beginning of the next evaporite cycle:

a — phenomena described in points 1 - 3

b — crystallization of fibrous gypsum in vugs which remained after dissolved halite

c — redolomitization of the shallow subsurface sediment

Subaerial exposure of the sediment need not occur over the whole of the pond bottom surface and usually it did not occur in this way. Depending on the lowering of the water table, more and more wide areas of the pond bottom were exposed. Drying of microbial mats, forming of desiccation cracks, tepees and alveolar structures, and crystallization of discoidal gypsum and displacive halite took place only in peripheric, subaerially exposed areas. In central parts of the pond, subaqueous conditions still existed and lime mud deposition and pelletization took place together with crystallization of needle-shaped and vertically oriented gypsum. The filling of the pond with sea water differed during flooding, which together with evaporation controlled facies distribution. Cavernous zones characterized by the occurrence of discoidal gypsum and displacive halite were developed mainly in peripheric parts of the pond where intensive evaporation occurred.

REFERENCES

Ahlburg, J., 1906. Die Trias im sudlichen Oberschlesien. *Abh. König. Preuss. Geol. Landesanstalt u. Bergakademie, N.F.,* 50: 1 – 163.

Aitken, J. D., 1967. Classification and environmental significance of cryptalgal limestones and dolomites with illustrations from the Cambrian and Ordovician of Southwestern Alberta. *J. Sedim. Petrol.,* 37: 1163 – 1178.

Arbey, F., 1980. Les formes et l'identification des evaporites dans les formations silicifiees. *Bull. CRE, Prod. Elf-Aquitaine,* 4/1: 309 – 365.

Arthurton, R. S., 1973. Experimentally produced halite compared with Triassic layered halite-rock from Cheshire, England. *Sedimentology,* 20: 145 – 160.

Assereto, R. L. A. M. & Kendall, C. G. S. C., 1977. Nature, origin and classification of peritidal tepee structures and related breccias. *Sedimentology,* 24: 153 – 210.

Assmann, P., 1913. Ein Beitrag zur Gliederung des Oberen Buntsandsteins im östlichen Oberschle-

sien. *Jb. Königl. Preuss. Geol. Landesanstalt*, 34, T. I, H. 3: 658 – 671

Assmann, P., 1933. Die Stratigraphie der oberschlesischen Trias. T. I – Der Buntsandstein. *Jb. Preuss. Geol. Landesanstalt*, 53: 731-757.

Back, W., Hanshaw, B. B., Plumer, L. N., Rahn P. H., Rightmire, C. T. & Rubin M., 1983. Process and rate of dedolomitization: Mass transfer and C dating in a regional carbonate aquifer. *Bull. Geol. Soc. Amer.*, 94: 1415 – 1429.

Bathurst, R. G. C., 1975. *Carbonate sediments and their diagenesis*. Elsevier, 2nd ed., Amsterdam, 658 pp.

Beales, F. W., 1965. Diagenesis in pelleted limestones. In: Pray, L. C., Murray, R. C. (eds), *Dolomitization and limestone diagenesis: a Symposium*. Soc. Econ. Paleont. Mineral. Spec. Publ., 13: 49 – 70.

Benkes, N. J., Lowe, D. R., 1989. Environmental control on diverse stromatolite morphologies in the 3000 Myr Pongola Supergroup, South Africa. *Sedimentology*, 36: 383 – 397.

Bustillo, M. A. & Diaz Molina, M., 1980. Silex "tobaceos" en el Mioceno inferior continental (provincia de Cuenca). Un ejemplo de silificaciones de paleosuelos en ambiente de lago-playa. *Bol. R. Soc. Esp., Hist. Nat. (Geol.)*, 78: 227 – 241.

Butler, G. P., 1969. Modern evaporite deposition and geochemistry of coexisting brines, the sabkha, Trucial Coast, Arabian Gulf. *J. Sedim. Petrol.*, 39: 70 – 89.

Carballo, J. D., Land, L. S. & Miser, D. E., 1987. Holocene dolomitization of supratidal sediments by active tidal pumping. *J. Sedim. Petrol.*, 57: 153 – 165.

Carozzi, A. V., 1962. Observations on algal biostromes in the Great Salt Lake, Utah. *J. Geol.*, 70: 246 – 252.

Carozzi, A. V., 1972. *Microscopic Sedimentary Petrography*. Krieger Comp., New York.

Chafetz, H. S., 1986. Marine peloids: a product of bacterially induced precipitation of calcite. *J. Sedim. Petrol.*, 56: 812 – 817.

Choquette, P. W. & Pray, L. C., 1970. Geologic nomenclature and classification of porosity in sedimentary carbonates. *Bull. Am. Ass. Petrol. Geol.*, 54: 207 – 250.

Chowns, T. M. & Elkins, J. E., 1974. The origin of quartz geodes and cauliflower cherts through the silicification of anhydrite nodules. *J. Sedim. Petrol.*, 44: 885 – 903.

Cloud, P. E., Jr, 1962. Environment of calcium carbonate deposition west of Andros Islands, Bahama. *Geol. Surv. Prof. Paper*, 350, 138 pp.

Cody, R. D., 1979. Lenticular gypsum: occurrences in nature and experimental determinations of effects of soluble plant material on its formation. *J. Sedim. Petrol.*, 49: 1015 – 1028.

Deicha, G., 1943. Genese et facies du gypse. *Bull. Soc. franc. Miner.*, 66: 153 – 160.

Dickson, J. A. D., 1966. Carbonate identification and genesis as revealed by staining. *J. Sedim. Petrol.*, 36: 491 – 505.

Doktorowicz-Hrebnicki, S., 1935. *Arkusz Grodziec. Mapa szczegolowa Polskiego Zagłębia Węglowego. Objaśnienia. z. 2.*, (In Polish only), Państw. Inst. Geol., Warszawa, 218 pp.

Dżułyński, S. & Kubicz A., 1971. Recrystallized and disaggregated limestones in the Triassic of Silesia. *Rocz. Pol. Tow. Geol.*, 41: 519 – 530.

Eck, H., 1865. *Über die Formationen des bunten Sandsteins und des Muschelkalks in Oberschlesien und ihre Versteinerungen.* Berlin, 50 pp 1 – 150.

Esteban, M., 1974. Caliche textures and Microcodium. *Bull. Soc. Geol. Italiana*, 92: 105 – 125.

Esteban, M. & Klappa, C. F., 1983. Subaerial Exposure Environment. In: Scholle, P. A., Bebout, D. G. & Moore, C. H. (eds), *Carbonate Depositional Environments*. Am. Ass. Petr. Geol., Tulsa, p. 1 – 54.

Evamy, B. D., 1967. Dedolomitization and the development of rhombohedral pores in limestones. *J. Sedim. Petrol.*, 37: 1204 – 1215.

Evamy, B. D., 1969. The precipitational environment and correlation of some calcite cements deduced from artificial staining. *J. Sedim. Petrol.*, 39: 787 – 793.

Folk, R. L. & Pittman, J. S., 1971. Length-Slow Chalcedony. A new testament for vanished evaporites. *J. Sedim. Petrol.*, 41: 1045 – 1058.

Folk, R. L. & Land, L. S., 1975. Mg/Ca ratio and salinity: two controls over crystallization of

dolomite. *Bull. Am. Ass. Petr. Geol.*, 59: 60 – 68.

Friedman, G. M., 1959. Identification of carbonate minerals by staining methods. *J. Sedim. Petrol.*, 29: 87 – 97.

Friedman, G. M., 1965. Terminology of crystallization textures and fabrics in sedimentary rocks. *J. Sedim. Petrol.*, 35: 643 – 655.

Friedman, G. M. & Sanders, J. E., 1967. Origin and occurrence of dolostones. In: Chillingar, H. J., Bissel, H. J. & Fairbridge, R. W. (eds), *Carbonate Rocks. Origin, Occurrence and Classification.* Elsevier, Amsterdam, pp 267 – 348.

Friedman, G. M. & Krumbein, W. E. (eds), 1985. Hypersaline ecosystems – The Gavish Sabkha. *Ecological Studies*, 53, 484 pp.

Geeslin, J. H. & Chafetz, H. S., 1982. Ordovician Aleman ribbon cherts: an exemple of silicification prior to carbonate lithification. *J. Sedim. Petrol.*, 52: 1283 – 1294.

Gerdes, G. & Krumbein, W. E., 1987. Biolaminated Deposits. *Lecture Notes in Earth Sciences*, 9, 183 pp.

Gornitz, V. M. & Schreiber, B. C., 1981. Displacive halite hoppers from the Dead Sea: some implications for ancient evaporite deposits. *J. Sedim. Petrol.*, 51: 787 – 794.

Groot, K., de, 1967. Experimental dedolomitization. *J. Sedim. Petrol.*, 37: 1216 – 1220.

Groot, K., de, 1973. Geochemistry of tidal flat brines at Umm Said, SE Qatar, *Persian Gulf.* In: Purser, B. H. (ed.), The Persian Gulf. Springer, Berlin, pp. 377-394.

Hardie, L. A., 1987. Dolomitization: a critical view of some current views. *J. Sedim. Petrol.*, 57: 109 – 119.

Hardie, L. A. & Eugster, H. P., 1971. The depositional environment of marine evaporites: a case for shallow clastic accumulation, *Sedimentology*, 16: 187 – 220.

Horodyski, R. J., 1977. Lyngbya mats at Laguna Mormona, Baja California, Mexico: comparison with Proterozoic stromatolites. *J. Sedim. Petrol.*, 47: 1305 – 1320.

Karcz, I. & Zak, I., 1987. Bedforms in salt deposits of the Dead Sea brines. *J. Sedim. Petrol.*, 57: 723 – 735.

Kendall, C. G. S. C. & Skipwith, P. A. d E., 1967. Holocene shallow water carbonate and evaporite sediments of Khor al Bazam, Abu Dhabi, South West Persian Gulf. *Bull. Am. Ass. Petrol. Geol.*, 53: 841 – 869.

Kendall, C. G. S. C. & Skipwith, P. A. d E., 1968. Recent algal mats of a Persian Gulf lagoon. *J. Sedim. Petrol.*, 38: 1040 – 1058.

Kendall, C. G. S. C. & Warren, J., 1987. A review of the origin and setting of tepees and their associated fabrics. *Sedimentology*, 34: 1007 – 1027.

Kirov, G. K., 1980. Growth forms of gypsum crystals grown by isothermal evaporation of solutions. *Geochim. Miner. Petrol.*, 12: 18 – 28.

Klappa, C. F., 1980. Rhizolits in terrestial carbonates; classification, recognition, genesis and significance. *Sedimentology*, 27: 613 – 629.

Kwiatkowski, S., 1991. Origin of the chert laminae and silico-calcareous nodules in the uppermost Röth Cavernous Limestone (Upper Silesia). *Acta Geol. Polon.* (in press)

Lasemi, Z., Boardman, M. R. & Sandberg, P. A., 1989. Cement origin of supratidal dolomite, Andros Islands, Bahamas. *J. Sedim. Petrol.*, 59: 249 – 257.

Longman, M. W., 1980. Carbonate diagenetic textures from near-surface diagenetic environments. *Bull. Am. Ass. Petrol. Geol.*, 64: 461 – 487.

Lowenstein, T. K. & Hardie, L. A., 1985. Criteria for the recognition of salt-pan evaporites. *Sedimentology*, 32: 627 – 644.

MacIntyre, I. G., 1985. Submarine cements. The peloidal question. In: Schneidermann, N. & Harris, P. M. (eds), *Carbonate Cements. Soc. Econ. Paleont. Miner. Spec. Publ.*, 36: 109 – 116.

MacKee, E. D. & Gutschick, R. C., 1969. History of Redwall Limestone of northern Arizona. *Mem. Geol. Soc. Am.*, 114: 1 – 726.

Maglione, G., 1979. Un exemple de sedimentation continentale actuelle. Le bassin tchadien. In: *Depots evaporitiques. Chambre syndicale de la recherche et de la production du petrole et du gaz naturel.*, pp 5-9.

Mazzullo, S. J. & Birdwell, B. A., 1989. Syngenetic formation of grainstones and pisolites from fenestral carbonates in peritidal settings. *J. Sedim. Petrol.*, 59: 605 – 611.

Milliken, K. L., 1979. The silicified evaporite syndrome – two aspects of silicification history of former evaporite nodules from Southern Kentucky and Northern Tennessee. *J. Sedim. Petrol.*, 49: 245 – 256.

Park, R., 1976. A note on the significance of lamination in stromatolites. *Sedimentology*, 23: 379 – 393.

Patterson, R. J. & Kinsman, D. J. J., 1982. Formation of diagenetic dolomite in coastal sabkha along Arabian (Persian) Gulf. *Bull. Am. Ass. Petrol. Geol.*, 66: 28 – 43.

Peryt, T. M., 1984. Sedimentation and early diagenesis of the Zechstein Limestone in western Poland. (In Polish, with English summary), *Pr. Inst. Geol.*, 109: 1 – 80.

Podemski, M., 1973. Dedolomitization of the Zechstein Carbonates in the Region of Lubin. (In Polish, with English summary), *Kwart. Geol.*, 17: 487 – 496.

Purser, B. H. & Evans, G., 1973. Regional sedimentation along the Trucial Coast, SE Persian Gulf. In: Purser, B. H., (ed), *The Persian Gulf.* Springer, Berlin, pp. 211 – 231.

Schreiber, B. C. & Kinsman, D. J. J., 1975. New observations on the Pleistocene evaporites of Montallegro, Sicily and modern analog. *J. Sedim. Petrol.*, 45: 469 – 479.

Schreiber, B. C., Tucker, M. E. & Till, R., 1986. Arid shore-lines and evaporites. In: Reading, H. G., (ed), *Sedimentary environments and facies.* Blackwell Scient. Publ., Oxford, 2nd ed., pp. 189 – 228.

Shinn, E. A., 1968. Practical significance of birdseye structures in carbonate rocks. *J. Sedim. Petrol.*, 38: 215 – 223.

Shinn, E. A., Lloyd, R. M. & Ginsburg, R. N., 1969. Anatomy of a modern carbonate tidal flat, Andros Island, Bahamas. *J. Sedim. Petrol.*, 39: 1202 – 1228.

Shinn, E. A., 1973. Recent intertidal and nearshore carbonate sedimentation around rock highs, E Qatar, Persian Gulf. In: Purser, B. H., (ed), *The Persian Gulf.* Springer, Berlin, pp. 193 – 198.

Shinn, E. A., 1983a. Tidal flat environment. In: Scholle, P. A., Bebout, D. G. & Moore, C. H., (eds), *Carbonate Depositional Environments. Am. Ass. Petrol. Geol. Mem.*, 33: 171 – 210.

Shinn, E. A., 1983b. Birdseyes, fenestrae, shrinkage pores and loferites: a reevaluation. *J. Sedim. Petrol.*, 53: 619 – 628.

Sibley, D. F. & Gregg, J. M., 1987. Classification of dolomite rock textures. *J. Sedim. Petrol.*, 57: 967 – 975.

Siedlecki, S., 1949. Problems of stratigraphy of marine Triassic in the Cracow area. *Rocz. Pol. Tow. Geol.*, 18: 191 – 272.

Siedlecki, S., 1952. Utwory geologiczne obszaru pomiędzy Chrzanowem a Kwaczałą. (In Polish only), *Biul. Państ. Inst. Geol.*, 60: 1 – 230.

Southgate, P. N., 1982. Cambrian skeletal halite crystals and experimental analogues. *Sedimentology*, 29: 391 – 408.

Steinen, R. P., 1974. Phreatic and vadose diagenetic modification of Pleistocene limestone; petrographic observations from subsurface of Barbados, West Indies. *Bull. Am. Ass. Petrol. Geol.*, 58: 1008 – 1024.

Theriault, F. & Hutcheon, I., 1987. Dolomitization and calcitization of the Devonian Grosmont Formation, North Alberta. *J. Sedim. Petrol.*, 57: 955 – 966.

Vai, G. B. & Ricci-Lucchi, F., 1977. Algal crusts, autochthonous and clastic gypsum in a cannibalistic evaporite basin: a case history from the Messynian of Northern Appenines. *Sedimentology*, 24: 211 – 244.

Warren, J. K., 1982. The hydrological setting, occurrence and significance of gypsum in Late Quaternary salt lakes in South Australia. *Sedimentology*, 29: 609 – 639.

Warren, J. K. & Kendall, C. G. S. C., 1985. Comparision of sequences formed in marine sabkha (subaerial) and salina (subaqueous) settings – modern and ancient. *Bull. Am. Ass. Petrol. Geol.*, 22: 953 – 983.

West, I. M., 1964. Evaporite diagenesis in the lower Purbeck Beds of Dorset. *Proc. Geol. Soc. Yorkshire.* 34: 315 – 330.

West, I. M., Brandon, A. & Smith, M., 1968. A tidal flat evaporitic facies in the Visean of Ireland. *J. Sedim. Petrol.*, 38: 1079 – 1093.

Streszczenie

SEDYMENTACJA I WCZESNA DIAGENEZA WAPIENIA JAMISTEGO (NAJWYŻSZY DOLNY TRIAS) REGIONU ŚLĄSKO-KRAKOWSKIEGO, POLSKA

Adam Bodzioch & Stanisław Kwiatkowski

Poziom wapienia jamistego występuje na granicy dolnego i środkowego triasu w regionie śląsko-krakowskim. Utworzony jest on głównie z dedolomitu i peloidowych wapieni ziarnistych, z licznymi pseudomorfozami po gipsie i halicie, bułami krzemionkowymi, matami algowymi, strukturami tepee, teksturami fenestralnymi, ripplemarkami falowymi i śladami erozji śródformacyjnej. Te cechy oraz mikrofacje wapienne wskazują na sedymentację w płytkich zbiornikach supralitoralnych, w przemiennych okresach silnej ewaporacji i okresach zasilania wodami morskimi.

W okresach ewaporacyjnych osadzał się muł wapienny podlegający szybkiej peletyzacji, przy rosnącym zasoleniu krystalizował gips, anhydryt i halit oraz występowała powierzchniowa dolomityzacja i selektywna sylifikacja mat algowych i konkrecji anhydrytowych.

W okresach dopływu wod morskich następowała erozja i osadzanie allochtonicznego materiału, złożonego z peloidów, onkoidów, bioklastów i detrytycznego kwarcu. W wyniku spadku temperatury, zasolenia i pH miało miejsce rozpuszczanie minerałów solnych, kalcytyzacja osadu i wytrącanie krzemionki.

EXPLANATION OF PLATES

Plate I

1 — Oval pits in a layer of crystalline limestone. Scale is 10 cm
2 — Cellular limestone. Vertical and diagonal walls (arowed) are built of calcitic pseudomorphs after discoidal gypsum. Scale is 1 cm
3 — Calcitic pseudomorphs after fibrous gypsum. Scale is 1 cm
4 — Cellular limestone. Walls of cells are built of dedolomite which remained between primary crystals of halite now removed. The arrow shows a calcitic pseudomorph after idiomorphic crystal of halite. Scale is 1 cm
5 — Cells after dissolved and removed evaporitic minerals. Scale is 1 cm
6 — Intracrystalline porosity within a relict of the crystal of displacive halite shown in Pl. I, fig. 4 (center, right). Scale is 0.5 cm

Plate II

1 — Peloidal grainstone with rhomboidal outlines of intergranular pores. Scale is 0.1 cm
2 — *Glomospira* sp. in non pelletted sediment. Scale is 0.1 mm
3 — ?*Endothyra* sp. at the boundary between pelletted and non pelletted laminae. Scale is 0.1 mm
4 — Undeterminate ostracod. Scale is 0.1 mm
5 — Calcitic pseudomorphs after dolomite around peloids. Scale is 0.02 mm
6 — Birdseye structure in poorly pelletted sediment. Scale is 1 mm

Plate III

1 — Calcitized sucrosic dolomite with relicts of dissolved dolomite (*black, cloudy areas*). The relict of an oncoid is shown by the arrow. Scale is 0.1 mm
2 — Relicts of peloids in dedolomite. Scale is 0.1 mm
3 — Calcitic pseudomorphs after euhedral crystals of dolomite in large crystals of calcite. Scale is 0.1 mm
4 — Relict of a specimen of *Glomospira* sp. Scale is 0.1 mm
5 — Relicts of ostracod tests (arrowed) and pseudomorphs after needle-shaped crystals of gypsum (rightside them). Scale is 0.1 mm
6 — Calcitized fish-squama. Scale is 0.1 mm

Plate IV

1 — Alveolar texture; direct microphotograph from a thin section. Scale is 1 cm
2 — Boundary between autochthonous dedolomitized sediment (*lower part of the photograph*) and allochthonous lamina (*upper part of the photograph*) abundant in grains of detrital quartz (*arrows*). Scale is 0.1 mm
3 — Pseudomorphs after anhydrite laths. Scale is 0.1 mm
4 — Pseudomorphs after small needle-shaped crystals of gypsum dispersed within the sediment. In lower part of the photograph, erosional surface is visible. Scale is 0.1 mm

Plate V

1 — Pseudomorphs after discoidal crystals of gypsum, topside view. Scale is 1 cm
2 — Pseudomorphs after redeposited hopper crystals of halite at the bottom surface of wave ripples. Scale is 1 cm

Plate VI

1 — Calcitic pseudomorph after a hopper crystal of halite. Scale is 1 cm
2 — Zoned structure of a pseudomorph after hopper crystal of halite. Direct microphotograph from thin section; *black areas* – blocky sparite, *white areas* – dedolomite. Scale is 1 cm
3 — Magnification of the crystal shown in Pl. VI, fig. 2, crossed nicols. Large sparite crystals (*lower part*) extinguish light together with incorporated dedolomite zones. Scale is 0.1 mm
4 — Calcitized laminated crust. Laminae of pseudomorphs after vertically oriented gypsum separated by thin micritic coatings. Scale is 0.5 mm
5 — Pseudomorphs after dissolved crystals of displacive halite. Scale is 5 cm
6 — The same specimen as in fig. 5, side view. Scale is 5 cm

Plate VII

1 — Silicified anhydrite nodules (*arrow*) in laminated limestone. Explanation in text
2 — "Pile of bricks" texture in silicified anhydrite nodule. Scale is 0.1 mm

Plate VIII

1 — Cryptalgal fabric with a nodular body. Scale is 1 cm
2 — Well preserved algal mat. The cavity in the upper part is filled with crystalline silt (*arrow*),
       granular and blocky sparite. The cavity in the lower part is filled with silica (*arrow*) and
       blocky sparite (*left side*). Algal filament is also filled with calcitic crystalline silt.
       Scale is 0.1 mm
3 — Collapse breccia within an internal cavity of the algal mat. Scale is 0.1 mm
4 — Cracked upper surface of algal laminae. The fissure is filled with granular sparite. Scale is
       0.1 mm

Plate IX

Silicified algal mat on the top surface of a limestone bed

Plate X

Siliceous plates surrounded by rings. Silicified algal mat

Plate XI

1 — Collapse breccia, hand sample. Scale is 1 cm
2 — Thin section of the sample shown in fig. 1, direct microphotograph. Scale is 1 cm
3 — Magnification of the part of fig. 2 (*encircled*) showing early granular sparite rim cement and
       late, postcompactional blocky sparite cement. Scale is 1 mm
4, 5 — Tepee structures. Scale is 5 cm
6 — *Planolites*. Scale is 1 cm

Plate XII

1 — *A* – cavernous limestone without detritic quartz; *B* – chert; *C* – limestone with detritic
       quartz, without vugs
2 — Silico-calcareous nodules. *White* – silica, *gray* – limestone
3 — Tubular siliceous nodule. *White* – silica, *gray* and *black* – limestone. Scale is 1 cm

Pl. I

Pl. II

Pl. IV

Pl. XI